Molecular Crystals and Liquid Crystals

ISSN: 1542-1406 (Print) 1563-5287 (Online) Journal homepage: http://www.tandfonline.com/loi/gmcl20

Synthesis and characterization of red phosphorescent iridium(III) complexes based on electron-acceptor modulation of main ligand for high efficiency organic light-emitting diodes

Sang-Yong Park, Hyun-Kyung Kim & Dong-Myung Shin

To cite this article: Sang-Yong Park, Hyun-Kyung Kim & Dong-Myung Shin (2016) Synthesis and characterization of red phosphorescent iridium(#) complexes based on electron-acceptor modulation of main ligand for high efficiency organic light-emitting diodes, Molecular Crystals and Liquid Crystals, 636:1, 38-44, DOI: 10.1080/15421406.2016.1200941

To link to this article: http://dx.doi.org/10.1080/15421406.2016.1200941

Published online: 01 Nov 2016.

MOLECULAR CRYSTALS AND LIQUID CRYSTALS
2016, VOL. 636, 38–44
http://dx.doi.org/10.1080/15421406.2016.1200941

Taylor & Francis
Taylor & Francis Group

Synthesis and characterization of red phosphorescent iridium(III) complexes based on electron-acceptor modulation of main ligand for high efficiency organic light-emitting diodes

Sang-Yong Park[a], Hyun-Kyung Kim[b], and Dong-Myung Shin[a]

[a]Department of Chemical Engineering, Hong-ik University, Seoul, Korea; [b]Korea Institute for Curriculum and Evaluation, Seoul, Korea

ABSTRACT

A new series of red phosphorescent iridium(III) complexes, (PT-TFP)2Ir(tmd), (PT-P)2Ir(tmd), and (PT-MP)2Ir(tmd) were synthesized for highly efficient red emitter of the organic light-emitting diodes (OLEDs). The main ligands consisted of electron-donor (phenanthren) and electron-acceptor (trifluoromethyl pyridine, pyridine, and methyl pyridine) were synthesized by Suzuki coupling reaction. The iridium(III) complexes based on main ligands and 2,2,6,6-tetramethyl-3,5-heptanedione(tmd) ancillary ligand were synthesized by Nonoyama reaction. Their luminescence properties were investigated by UV-visible spectroscopy and photoluminescence (PL) spectroscopy. The OLEDs devices were manufactured by vacuum deposition and These OLEDs devices were characterized by investigation of current density-voltage-luminance (J-V-L), current efficiency, power efficiency, external quantum efficiency (EQE), EL spectrum. The Ir(III) complexes will be used as a solution process dopant for the hybrid OLED devices.

KEYWORDS

red dopant; iridium(III) complexes; phosphorescent organic light-emitting diodes

1. Introduction

Active matrix phosphorescence organic light emitting diodes (AMPhOLED) attracting attention as the next generation display have been evolving into high dfficiency, high definition, large area, and flexible display. OLED has a lot of difficulties in the development process because materials of OLED are required to have ultra high purity than materials of other displays. But because of Lambertian reflectance characteristic, AMPhOLED has less visual stimuli and high illumination. Therefore It is more friendly human body[1–8].

In this paper, phosphorescent red dopants which are used as solution process was investigated. Red dopants are required to emit a red long-wavelength red light and high efficiency as the core of the light-emitting material at the same time. In this study, by combining the design of a phosphorescent iridium compound was studied for the implementation of a complete high-efficiency devices for reddish solution process was carried out basic research, which enables a large area device fabrication using less processes.

CONTACT Dong-Myung Shin shindm@hongik.ac.kr Department of Chemical Engineering, Hong-ik University, 94, Wausan-ro, Mapo-gu, Seoul 04066, Korea; Hyun-Kyung Kim kimhk@kice.re.kr Korea Institute for Curriculum and Evaluation, Jeongdong Bldg., 15-5, Jeong-dong, Jung-gu, Seoul 100-784, Korea.

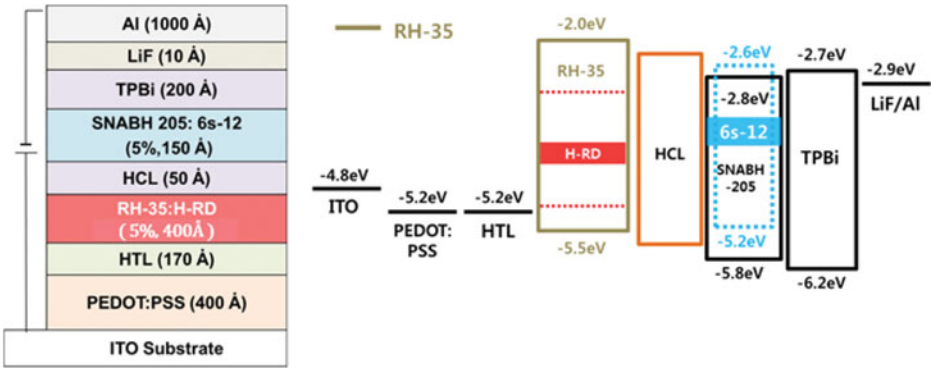

Figure 1. Device structure and energy band-gap of materials used in the device.

2. Experimental details

2.1. General information

All reagents and solvents were purchased from Aldrich Chemical Co., TCI, and Alpha Aesar, and they were used without further purification. All column chromatography was performed under a standard atmosphere using silica gel (230–400 mesh, Sigma-Aldrich). The 1H NMR spectra were measured using a UNITY-INOVA 500MHz Nuclear Magnetic Resonance Spectrometer of VARIAN. INC. in a deuterated chloroform solution. UV–visible absorption spectra were recorded on an Agilent 8453 UV–Visible spectrophotometer. Photoluminescence (PL) spectra were obtained using an LS55 fluorescence spectrometer. The current density-voltage (J-V) and luminance-voltage (L-V) data of OLEDs were measured by the Keithley SMU 238 and Minolta CS-100A, respectively. The OLED area was 4 mm2 for all the samples studied in this work. Electroluminescence (EL) spectra and CIE coordinates were obtained using a Minolta CS-2000 spectroradiometer.

2.2. Synthesis of the main ligands

4-methyl-2-(phenanthren-9-yl)pyridine (PT-MP). A mixture of phenanthren-9-ylboronic acid (1.00 g, 4.503 mmol), 2-bromo-4-methylpyridine (0.85 g, 4.954 mmol), tetrakis(triphenylphosphine)palladium (0.05 g, 0.045 mol, 1 mol%), potassium carbonate (15 ml, 2M aqueous solution), and tetrahydrofuran (30 mL) was headed under a nitrogen atmosphere at 80°C for 24 h. This reaction is the Suzuki coupling reaction. After the reaction, the mixture was cooled to room temperature for 1 h. The compound was extracted by liquid-liquid separation (water and dichloromethane). The compound was purified by a celite-silica gel filtration (solvent: toluene) and column chromatography on silica gel (eluent: hexane/ethyl acetate, 15:1). Yield: 98.9% (1.20 g); 1H NMR 500 MHz, CDCl3, δ), δ(ppm): 8.93 (d, J = 7.3 Hz, 2H), 8.44(s, 1H), 8.39(d, J = 6.7 Hz, 1H), 8.12 (d, J = 7.1 Hz, 2H), 7.96(s, 1H), 7.88(dd, J = 18.2 Hz, 2H), 7.82(dd, J = 19.1 Hz, 2H), 7.05(d, J = 5.3 Hz, 1H), 2.36(s, 3H).

2-(phenanthren-9-yl)pyridine (PT-P). A PT-P ligand was obtained from the reaction of phenanthren-9-ylboronic acid (1.00 g, 4.503 mmol) and 2-bromopyridin (0.78 g, 4.954 mmol) by Suzuki coupling. Yield: 99.1% (1.14 g); 1H NMR 500 MHz, CDCl3, δ), δ(ppm): 8.93(d, J = 7.3 Hz, 2H), 8.50(d, J = 7.8 Hz, 1H), 8.44(s, 1H), 8.12 (d, J = 7.1 Hz, 2H), 7.88

(dd, J = 18.2 Hz, 2H), 7.82(dd, J = 19.1 Hz, 2H), 7.51(dd, J = 14.7 Hz, 1H), 7.26(d, J = 4.8 Hz, 1H), 7.00(dd, J = 17.1 Hz, 1H).

2-(phenanthere-9-yl)-4-(trifluoromethyl)pyridine (PT-TFP). A PT-TFP ligand was obtained from the reaction of phenanthren-9-ylboronic acid (1.00 g, 4.503 mmol) and 2-bromo-4-(trifluoromethyl)pyridin (1.12 g, 4.954 mmol) by Suzuki coupling. Yield: 97.5% (1.42 g); 1H NMR 500 MHz, CDCl3, δ), δ(ppm): 8.93(d, J = 7.3 Hz, 2H), 8.44(s, 1H), 8.38(d, J = 6.9 Hz, 1H), 8.12 (d, J = 7.1 Hz, 2H), 8.06(s, 1H), 7.88(dd, J = 18.2 Hz, 2H), 7.82(dd, J = 19.1 Hz, 2H), 7.15(d, J = 5.9 Hz, 1H).

2.3. Synthesis of the cyclometalated iridium(III) μ-chloride-bridged dimer

Dimer [(PT-MP)$_2$IrCl]$_2$ diiridium(III). The cyclometalated iridium(III) μ-chloride-bridged dimer, [(PT-MP)2Ir(μ-Cl)]2 (II), was prepared using a slightly modified Nonoyama reaction step 1. Iridium(III) chloride hydrate (0.665 g, 2.228 mmol) and PT-MP (1.20 g, 4.45 mmol) were dissolved in a mixed solution of 2-ethoxyethanol and water (36 ml: 12 ml). The reaction was required under a nitrogen atmosphere. The mixture was refluxed overnight at 135°C. The solution was cooled to room temperature for 1 h. The crude product was purified via liquid-liquid separation (dichloromethane and water). The precipitation was collected by a vacuum evaporator. Yield: 98.7%.

Dimer [(PT-P)$_2$IrCl]$_2$ diiridium(III). The cyclometalated iridium(III) μ-chloride-bridged dimer, [(PT-P)$_2$Ir(μ-Cl)]$_2$ (II), was obtained from the reaction of iridium(III) chloride hydrate (0.667 g, 2.233 mmol) and PT-P (1.60 g, 4.465 mmol) by the Nonoyama reaction step 1. Yield: 97.3%.

Dimer [(PT-TFP)$_2$IrCl]$_2$ diiridium(III). The cyclometalated iridium(III) μ-chloride-bridged dimer, [(PT-TFP)$_2$Ir(μ-Cl)]$_2$ (II), was obtained from the reaction of iridium(III) chloride hydrate (0.656 g, 2.196 mmol) and PT-TFP (1.42 g, 4.392 mmol) by the Nonoyama reaction step 1. Yield: 95.5%.

2.4. Synthesis of the iridium(III) complexes (Scheme 1)

(PT-MP)$_2$Ir(tmd) complex: [(PT-MP)2Ir(μ-Cl)]2 (II) (1.68 g, 1.099 mmol), 2,2,6,6-tetramethyl-3,5-heptanedione (1.013 g, 5.495 mmol), and sodium carbonate (1.519 g, 10.99 mmol) were dissolved in 2-ethoxyethanol (67.20 ml) and refluxed under a nitrogen atmosphere overnight at 130°C. After cooling to room temperature for 2 h. The compound was extracted by liquid-liquid separation (water and dichloromethane). The compound was purified by a celite-silica gel filter (solvent: toluene) and column chromatography on silica gel (eluent: methanol/CH2Cl2, 1:40). The product was further purified by recrystallization to the Yield: 89.7%; 1H NMR (500 MHz, CDCl3, δ), δ(ppm): 8.62(dd, J = 29 Hz, 4H), 8.45(d, J = 9.9 Hz, 2H), 8.37(s, 2H), 7.62 (dd, J = 19.85 Hz, 4H), 7.50(t, J = 17.55 Hz, 2H), 7.24 (dd, J = 16.8 Hz, 2H), 6.62(t, J = 19.1 Hz, 2H), 6.53(d, J = 7.6 Hz, 2H), 6.37(d, J = 9.15 Hz, 2H), 5.38(s, 1H), 2.53(s, 6H), 0.859(s, 18H).

The (PT-P)$_2$Ir(tmd) complex was obtained from the reaction of [(PT-P)2Ir(μ-Cl)]2 (II) (1.60 g, 1.087 mmol) and 2,2,6,6-tetramethyl-3,5-heptanedione (1.001 g, 5.433 mmol) by the Nonoyama reaction step 2. Yield: 88.9%; 1H NMR (500 MHz, CDCl3, δ), δ(ppm): 8.62 (dd, J = 29 Hz, 4H), 8.44(d, J = 9.9 Hz, 2H), 8.37(s, 2H), 7.62 (dd, J = 19.85 Hz, 4H), 7.51(dd, J = 17.55 Hz, 2H), 7.24(dd, J = 16.8 Hz, 2H), 6.62(t, J = 19.1 Hz, 2H), 6.53(d, J = 7.6 Hz, 2H), 6.43(d, J = 8.2 Hz, 2H), 6.32(d, J = 9.15 Hz, 2H), 5.38(s, 1H), 0.859(s, 18H).

Table 1. Photophysical properties of Ir-complexes and the Device performance of solution-processed red phosphorescent OLEDs.

Red Dpants	Abs λ_{Max} (nm)	PL λ_{Max} (nm)	EL λ_{Max} (nm)	Current Efficiency (Ca/A)	Power Efficiency (lm/W)	External Quantum Efficiency (%)	Color Index
$(PT\text{-}MP)_2Ir(tmd)$	261 339 464	624	627	8.56[a], 5.9[b]	5.44[a], 2.66[b]	12.35[a], 8.48[b]	(0.67, 0.32)[c]
$(PT\text{-}P)_2Ir(tmd)$	267 316 466	627	630	5.52[a], 4.81[b]	4.05[a], 1.93[b]	9.52[a], 6.73[b]	(0.68, 0.32)[c]
$(PT\text{-}TFP)_2Ir(tmd)$	257 316 485	649	654	2.62[a], 2.01[b]	1.64[a], 0.90[b]	6.70[a], 4.42[b]	(0.43, 0.25)[c]

[a] Maximum efficiency; [b] Efficiency at 1,000 cd/m^2; [c] Color coordinates were obtained at 1,000 cd/m^2.

The $(PT\text{-}TFP)_2Ir(tmd)$ complex was obtained from the reaction of [(PT-TFP)2Ir(μ-Cl)]2 (II) (1.83 g, 1.049 mmol) and 2,2,6,6-tetramethyl-3,5-heptanedione (0.967 g, 5.245 mmol) by the Nonoyama reaction step 2. Yield: 82.2%; 1H NMR (500 MHz, CDCl3, δ), δ(ppm): 8.62(dd, J = 29 Hz, 4H), 8.37(s, 2H), 8.16(d, J = 7.9 Hz, 2H), 7.62 (dd, J = 19.85 Hz, 4H), 7.60(dd, J = 15.23 Hz, 2H), 7.24(dd, J = 16.8 Hz, 2H), 6.62(t, J = 19.1 Hz, 2H), 6.53(d, J = 7.6 Hz, 2H), 6.47(d, J = 9.15 Hz, 2H), 5.38(s, 1H), 0.859(s, 18H).

2.5. Device fabrication

To fabricate solution-processed OLED devices, 150-nm thick patterned indium-tin oxide (ITO) glasses covered by a bank layer with an open emission area of 4 mm^2 were used. The ITO glasses were cleaned in acetone and isopropyl alcohol with a sonication process and rinsed in deionized water. Then, ITO glass substrates were treated in UV-ozone to eliminate all the organic impurities from the previous fabrication processes. A PEDOT:PSS as a hole injection layer was spin-coated on ITO glass in an ambient condition and annealed at 120°C for 15 min in an inert atmosphere. Subsequently, HTL as a hole transport layer dissolved in chlorobenzene was spin-coated and cross-linked by a standard process. In the case of a red EML host, red dopants were dissolved in toluene to produce a 5 wt% solution, respectively. A red EML was spin coated and dried at 100°C for 10 min. All solution processes were performed in a nitrogen atmosphere at room temperature, except PEDOT:PSS. After spin coating of red EML, the hybrid-connecting layer, blue EML, and TPBI were thermally deposited at a vacuum condition under 10-7 Torr with 0.5 Å/s. Then, LiF and Al were deposited successively with 0.3 Å/s and 3 Å/s, respectively (Fig. 1).

3. Results and discussion

Figure 2 shows the UV-visible absorption and photoluminescence (PL) spectra of the Ir(III) complex dissolved in a Dichloromethane solution.

The main absorption bands are located in between 300 nm and 500 nm. The distinct vibronic features are assigned to the spin-allowed $^1\pi$-π^* transition of the ligands in the Ir(III) complexes. Due to the perturbation of the Ir(III) metal center, these transitions were shifted with respect to those of the free ligands. The absorption peaks in the region of 450 nm–600 nm can be assigned to the spin-allowed metal-ligand charge transfer band (^{1}MLCT) and the spin-forbidden metal-to-ligand (^{3}MLCT) transition. The absorption bands with peak wavelengths

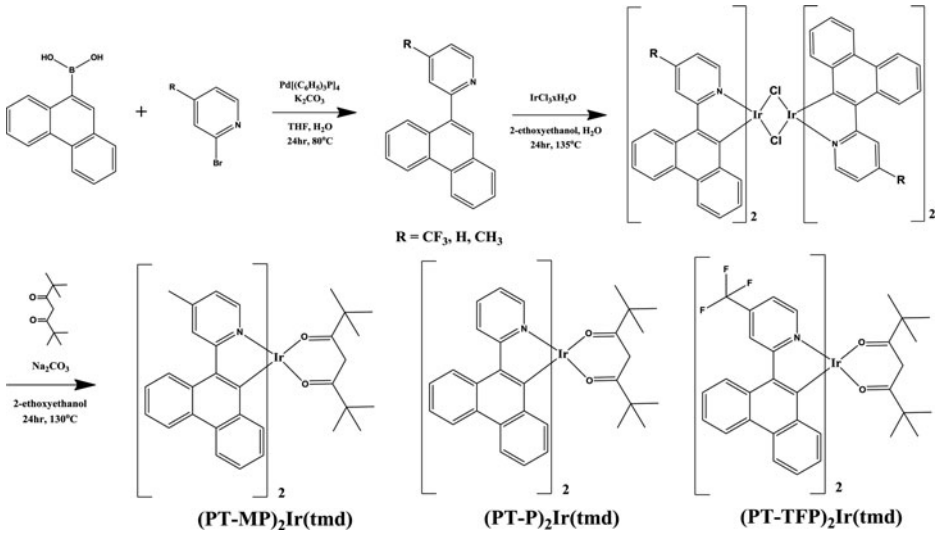

Scheme 1. Synthetic scheme and chemical structure of complexes.

around 600 nm suggest that the $S_0 \rightarrow {}^3$MLCT transition is greatly enhanced and becomes partially allowed due to strong spin-orbital coupling[9–12].

The PL spectra of complexes show the emission of red light with main peaks at 624–649 nm, as shown in Figure 2 (A). The phosphorescence peak wavelength can be tuned by aromatic amine moiety to the main ligand. Complexes with $-CH_3$ functional group of pyridine ring have a shorter phosphorescence wavelength than complexes with $-CF_3$, because the high electron-density of pyridine ring in the complexes increased the LUMO energy level.

Figure 2 (B) shows the EL emission spectra at a brightness of 1,000 cd/m^2 for the red PhOLEDs. The EL emission spectra of all the complexes are slightly (3–5 nm) red-shifted relative to the solution PL spectra. The devices give very deep red EL spectra with much narrower full width at half maximum (FWHM) compared to commercial OLED devices.

Figure 3 (a) shows the current density-voltage-luminance (J-V-L) curves of the fabricated red-phosphorescent OLEDs. At a constant voltage of 5.0 V, current density values of 0.10, 0.71 and 1.42 mA/cm^2 are observed in the fabricated PhOLEDs, respectively. The driving voltage

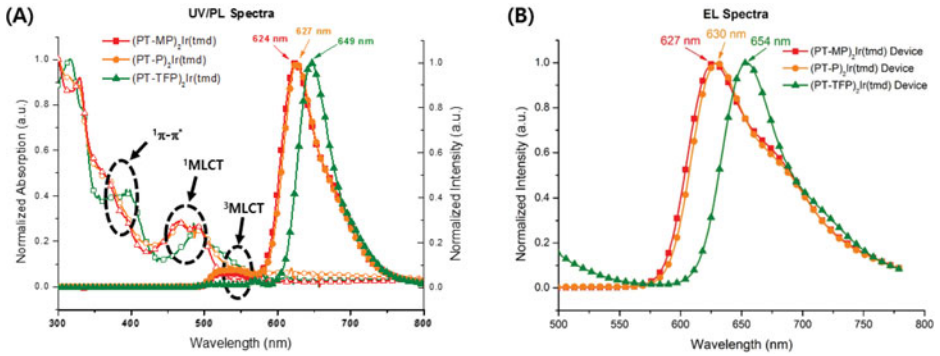

Figure 2. (A) UV/PL spectra of Ir-complexes and (B) Electroluminescence spectra of solution-processed red phosphorescent OLEDs.

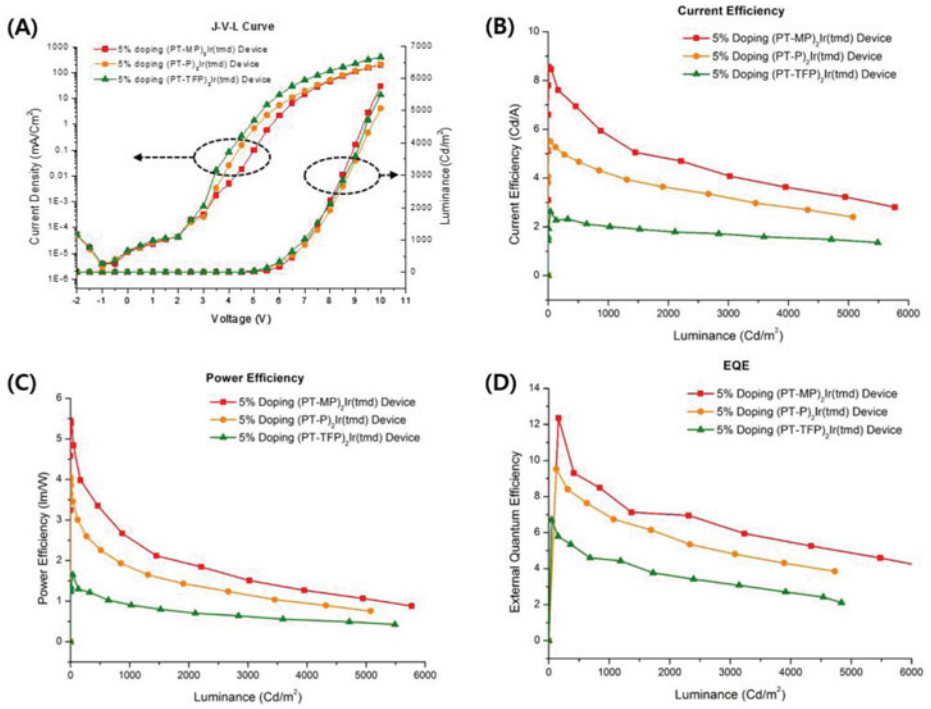

Figure 3. (A) J-V-L Characteristics of the red phosphorescent OLEDs (B) Current efficiency-luminance characteristics (C) Power efficiency-luminance characteristics (D) External quantum efficienty of fabricated phosphorescent OLEDs.

to reach 1,000 cd/m^2 is 7.14, 7.21 and 7.03V for devices, respectively. Also, a low turn-on voltage of 2.0 V for devices was observed.

The Photophysical properties of Ir-complexes and the device performance of solution-processed red PhOLEDs is summarized in Table 1. Figure 3. (B), (C) and (D) showed a similar trend of device performance. The (PT-MP)$_2$Ir(tmd) device showed a higher power efficiency, current efficiency, and external quantum efficiency than efficiency of other devices.

4. Conclusion

The –CF3 is an efficient electron-withdrawing group. Therefore, the electron density in the pyridine ring is decreased and the lowest unoccupied molecular orbital (LUMO) energy level is decreased. Therefore, the HOMO-LUMO energy gap of (PT-TFP)2Ir(tmd) is decreased and the emission wavelength is increased. Alternatively, the –CH3 functional group increases the electron density of the pyridine ring. Therefore, the LUMO energy level is increased and the HOMO-LUMO energy gap of (PT-MP)2Ir(tmd) is increased. When energy levels of all materials in devices was arranged properly and structure of dopants is similar, the phosphorescent red dopant having emission of low wavelength was proved to have a higher efficiency. Also, these dopants is highly proper for solution process.

Acknowledgments

This work was supported by the Technology Innovation Program (201210940004, Materials Development for 50-inches UD OLED TV Using Super Hybrid Process) and funded by the Ministry of

Knowledge Economy (MKE, Korea). We specially thank Professor M. C. Suh of Kyung-Hee University for the device performance experiments.

References

[1] Shin, D. M. (2014). *Sci. Adv. Mater. Appl.*, *6*, 1.
[2] Park, S. Y. et al. (2015). *Mol. Cryst. Liq. Cryst.*, *620*, 132.
[3] Lee, S. N. et al. (2014). *Mol. Cryst. Liq. Cryst.*, *599*, 112.
[4] Han, T. H. el al (2015). *J. Inform. Display.*, *16*, 71.
[5] Hyun, W. J. el al (2012). *J. Inform. Display*, *13*, 151.
[6] Wu, H. B. et al. (2011). *Adv. Mater.*, *21*, 4181.
[7] Yook, K. S. et al. (2010). *Adv. Mater.*, *22*, 4479.
[8] Song, M. K. et al. (2014). *Nanosci. Nanotechnol.*, *14*, 5495.
[9] You, Y. M. et al. (2009) *Dalton Trans.*, *8*, 1267.
[10] Hwang, J. Y. et al. (2015) *Dyes and Pigments*, *121*, 73.
[11] Tsuboi, T. et al (2008). *Jpn. J. Appl. Phys.*, *47*, 1266.
[12] Li, J. et al. (2005). *Inorg. Chem.*, *44*, 1713.